Supplemental Materials and Methods

Histological Analyses

To further verify our *in vivo* measurements, we performed hematoxylin eosin (H&E) staining and Ki-67 immunohistochemical staining on histological sections from arthritic and healthy ankles at days 1 (n=3 GPI, n=2 control), 3 (n=3 GPI, n=2 control) and 8 (n=5 GPI, n=3 control) after serum injection to correlate Ki-67 protein expression patterns with the ^{18}F-FLT-PET data. **Suppl. Figure 1B** shows the course of ankle swelling in the mice that were used for histological analysis. The mice were sacrificed and the joints from the hind and the front limbs were fixed in 4% formalin, decalcified and embedded in paraffin. Tissues were cut into 3-5 µm sections and stained with H&E following standard procedures (*1*). Immunohistochemistry was performed using an automated immunostainer (Ventana Medical Systems, Inc., Tucson, AZ, USA) according to the manufacturer's protocols for open procedures, with slight modifications. All slides were stained with a Ki-67-specific antibody (SP6; Thermo Fisher Scientific, MI, USA). Appropriate positive controls were used to confirm the adequacy of the staining.

Radiopharmaceutical

The radiopharmaceutical was synthesized from benzoyl-protected anhydrothyhmidine as described previously. Briefly, azeotropically dried ^{18}F-fluoride was reacted with the precursor. After removal of the protecting groups, the product was purified using preparative HPLC. The process yielded up to 10 GBq ^{18}F-FLT with a radiochemical purity >99% (*2*).

Autoradiography

For digital phosphor storage autoradiography analysis, ^{18}F-FLT was *i.v.* injected into the tail vein, and the animals were sacrificed 30 min later. The mice were kept anesthetized during the uptake period. Immediately after dissection, the ankles were embedded in an optimal-cutting-temperature compound (TissueTek; Sakura Finetek, Torrance, CA, USA) and frozen with a coolant spray. We analyzed on day 1 (GPI: n=2, control: n=1), day 3 (GPI: n=3, control: n=1), day 6 (GPI: n=2, control: n=2) and day 8 (GPI: n=2, control: n=2) the indicated numbers of mice. Autoradiography was performed with a Storage Phosphor Screen (Molecular Dynamics, Sunnyvale, CA, USA) from 20 µm sections of -20°C snap frozen arthritic and healthy ankles. The phosphor screens were scanned at a resolution of 50 µm/pixel with a STORM Phosphor-Imager (Molecular Dynamics) after 24 h of exposure time. For each mouse, standardized ROIs (47 x 54 pixels) were drawn around the hot spots of the left and the right ankles. For further analysis, the mean value of the analyzed autoradiogram for each ankle was used to calculate tracer uptake. The resulting images were analyzed using Image J Software .

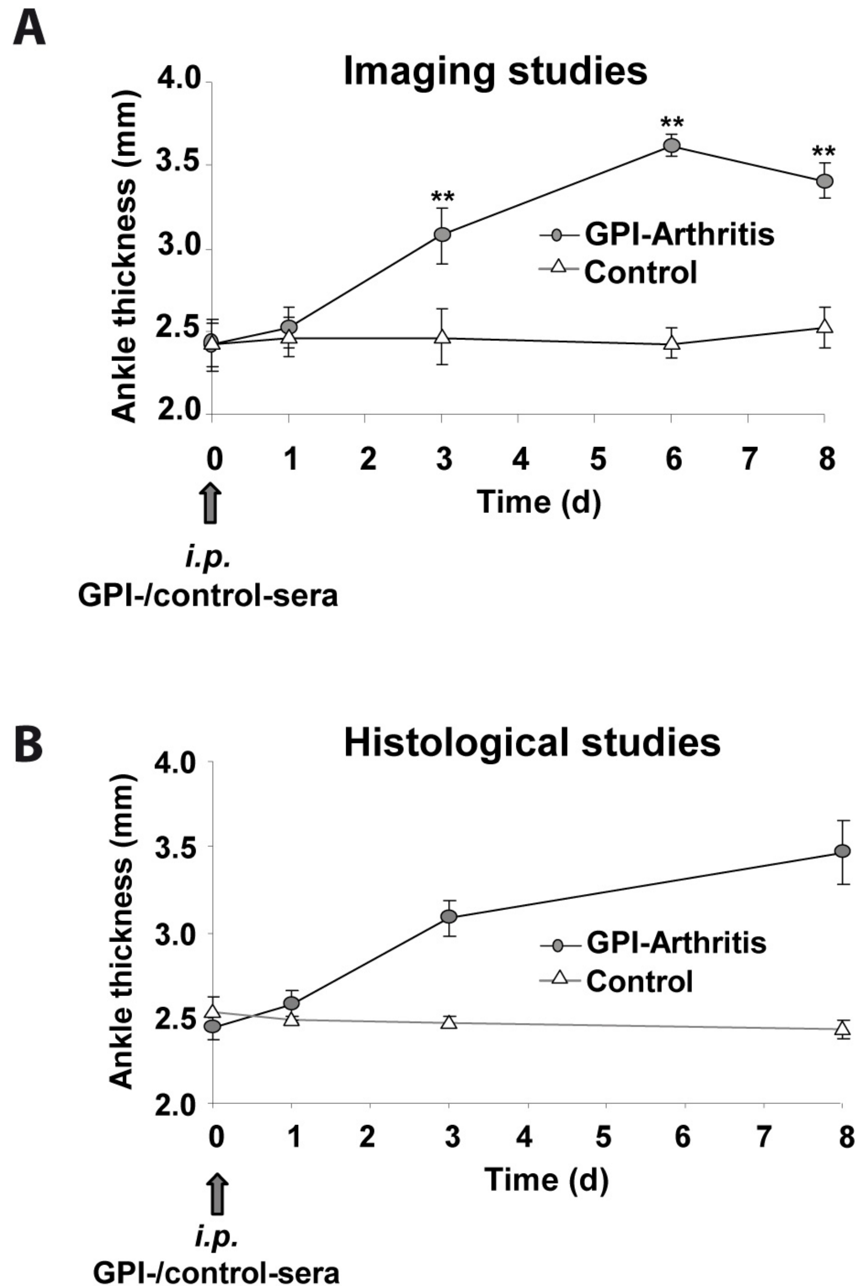

Supplemental Figure 1

(A) Course of ankle thickening in GPI- or control-serum injected mice which were investigated on days 1, 3, 6 and 8 by ^{18}F-FLT-PET, ^{18}F-FLT-PET/CT and ^{18}F-FLT-PET/MRI. **(B)** Course of ankle thickening in GPI- or control-serum injected mice which were sacrificed on days 1, 3, and 8 for histological and immunohistochemical analyses.

A

Day 1 Ratio	Day 3 Ratio	Day 6 Ratio	Day 8 Ratio
1.6	2.4	3.5	2.5

B

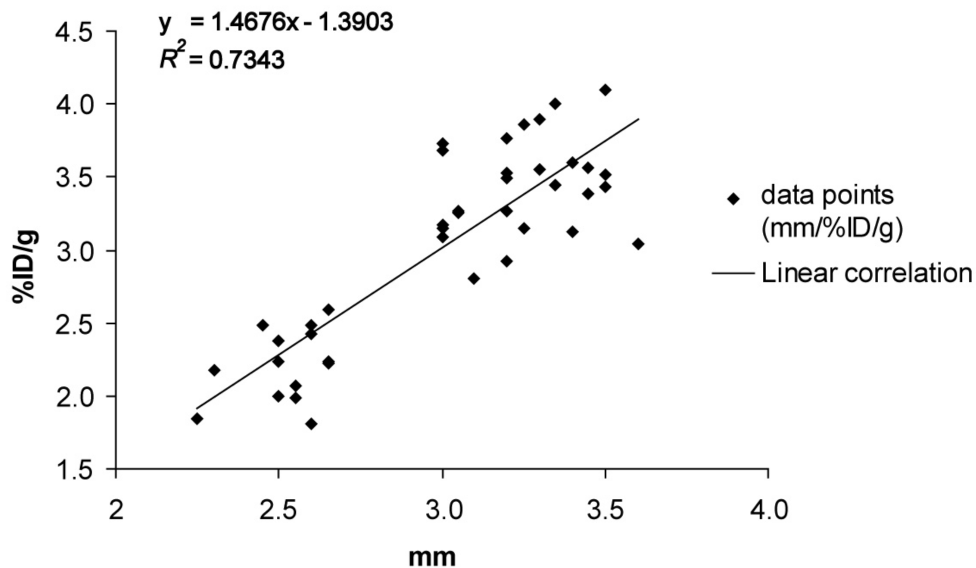

Supplemental Figure 2

(A) Ratios were calculated between the mean of %ID/g in GPI-arthritic and the mean of %ID/g in control ankles on days 1, 3, 6 and 8 after GPI- or control-serum injection. **(B)** We correlated ankle swelling (mm) and %ID/g from arthritic ankles at days 1, 3 and 8 after GPI-serum injection; the coefficient of determination was R^2=0.7343.

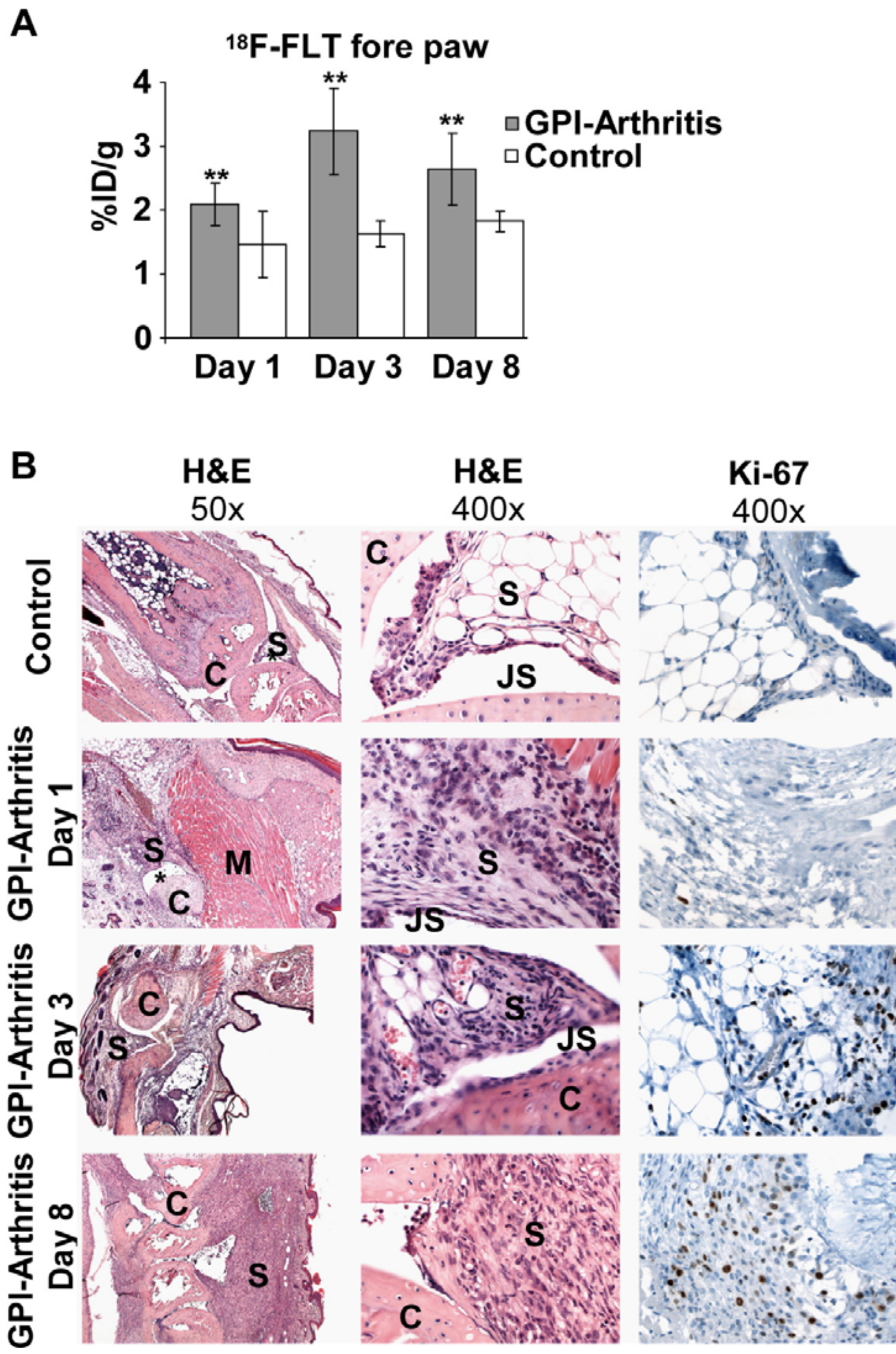

Supplemental Figure 3

(A) Quantification of the pooled dynamic and static ^{18}F-FLT-PET scans in arthritic and healthy fore paws (wrist, carpo-metacarpal, metacarpo-phalangeal and phalangeal joints) indicated as the mean %ID/g on days 1, 3 and 8 after GPI- or control-serum transfer. The ^{18}F-FLT-uptake values indicated increased accumulation

in the arthritic fore paws after GPI-serum injection (n=5-8) with the maximum uptake on day 3, indicating enhanced cell proliferation. The healthy fore paws (n=2-7) of control-serum-injected littermates exhibited constant ^{18}F-FLT tracer uptake at all corresponding time points. *P*-values < 0.05 were considered to be statistically significant. **(B)** H&E-stained slides from GPI-arthritic fore paws on days 1, 3 and 8 after GPI-serum transfer are shown at magnifications of 50X and 400X. Increasing accumulation of inflammatory cells, predominately neutrophils, ongoing pannus formation and joint destruction are evident. H&E-stained slides from the healthy fore paws of control-serum-injected mice revealed no signs of inflammation **(top row left and center panels)**. Ki-67 staining (400X) demonstrated an increasing number of highly proliferating cells between day 1 and day 8 after arthritis induction. The control fore paws showed few Ki-67-positive cells (C, cartilage; S, synovium; JS / *, joint space; T, tendon; M, muscle) **(right panels)**.

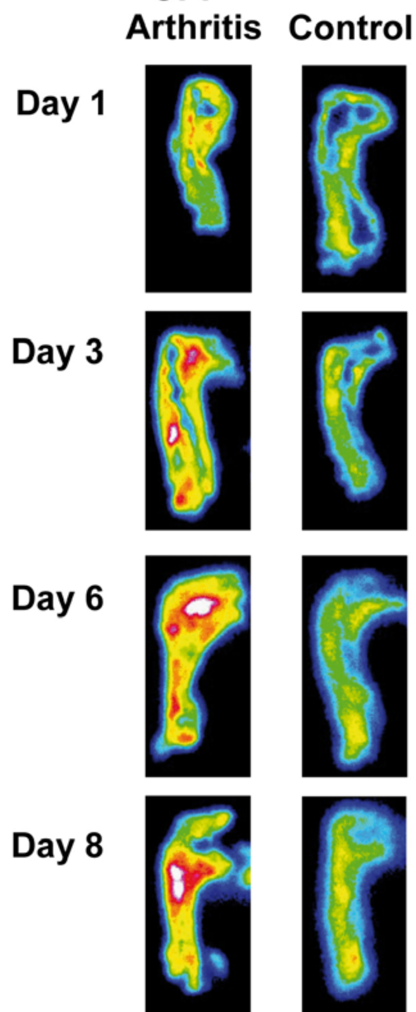

Supplemental Figure 4

^{18}F-FLT-autoradiography analyses confirm the *in vivo* ^{18}F-FLT-PET results. Representative ^{18}F-FLT-autoradiography analysis of slices from arthritic ankles of mice on days 1, 3, 6 and 8 after GPI-serum injection (left) and from healthy ankles of control-serum-injected mice (right). Increasing and homogeneous ^{18}F-FLT-tracer uptake in the arthritic ankles was observed starting on day 1 after arthritis induction. A further increase and ^{18}F-FLT-hot spots were observed beginning at day 3 after GPI-serum injection. The healthy control-ankles displayed a faint ^{18}F-FLT signal at all investigated time points.

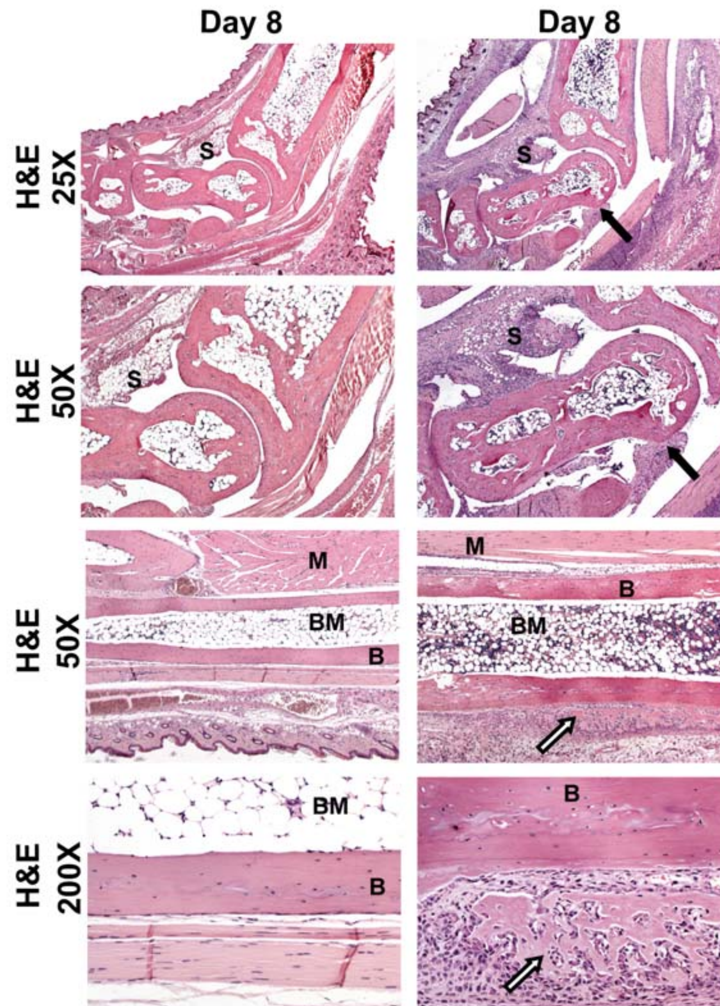

Supplemental Figure 5

H&E staining of GPI-arthritic ankles obtained after the final ^{18}F-FLT-PET/CT or ^{18}F-FLT-PET/MRI investigation that occurred 8 days after the GPI-serum injection. The slides revealed pannus formation and bone cortical erosion at the site of the tendon insertion (black arrow; magnifications of 25X and 50X; **right panel**). Additionally, strong reactive periosteal bone formation but no bone destruction was observed (white arrows; magnifications of 50X and 200X; **right panel**). H&E staining of healthy ankles of control-serum-injected mice revealed no signs of inflammation **(left panel**; magnifications of 25X, 50X and 200X). B, bone; BM, bone marrow; M, muscle; S, synovium.

References

1. Kneilling M, Hultner L, Pichler BJ, et al. Targeted mast cell silencing protects against joint destruction and angiogenesis in experimental arthritis in mice. *Arthritis Rheum.* Jun 2007;56(6):1806-1816.

2. Reischl G, Wei R, Ehrlichmann W, et al. Simplified, automated synthesis of 3'-[18F]Fluoro-3'-Deoxy-Thymidine ([18F]FLT) and simple method for metabolite analysis in plasma. *Radiochimica Acta.* 2006;94(8):447-4451.